

This is the accepted manuscript version of the contribution published as:

Saeidi, N., Kopinke, F.-D., Georgi, A. (2021):

Controlling adsorption of perfluoroalkyl acids on activated carbon felt by means of electrical potentials

Chem. Eng. J. **416** , art. 129070

The publisher's version is available at:

<http://dx.doi.org/10.1016/j.cej.2021.129070>

**Controlling adsorption of perfluoroalkyl acids on activated carbon felt by means of
electrical potentials**

Navid Saeidi, Frank-Dieter Kopinke, Anett Georgi*

Helmholtz Centre for Environmental Research – UFZ, Department of Environmental Engineering,

D-04318 Leipzig, Germany

Corresponding author e-mail: anett.georgi@ufz.de

Abstract

Electrosorption was investigated as an innovative approach for removal of perfluoroalkyl acids (PFAAs) from contaminated water. Direct electrical potentials were applied to conductive activated carbon felts (ACFs) for enhancing adsorption of PFAA anions under anodic polarization and facilitate desorption under cathodic polarization. Single point adsorption coefficients K_d of perfluorooctanoic acid (PFOA) at environmentally relevant concentrations vary between 650,000 L/kg at positive potentials and 14,800 L/kg at negative potentials, i.e. by a factor of 44. The differences were even higher (factor of 100) for perfluorobutanoic acid (PFBA). A first estimation of the achievable concentration factor for PFOA in a fixed-bed electrosorption unit with potential swings results in values ≥ 40 . This illustrates the great potential of electrosorption as pre-concentration approach which can be synergistically combined to subsequent PFAAs destruction technologies such as electrooxidation for concentrate treatment. The initial cyclic experiments at +500 mV/-1000 mV vs. Ag/AgCl revealed a decline in performance of the electrosorption cell over prolonged polarization times. Information on potential of zero charge (E_{PZC}) of the ACFs was used to select milder potential swings, e.g. $-100 \text{ mV} < E_{PZC} = +75 \text{ mV} < +300 \text{ mV}$ which significantly improved stability in a ten cycle electroadsorption/-desorption experiment over 1000 h operation time. The weak impact of competitive inorganic ions on electrosorption of PFBA and PFOA and a small effect of variable pH values indicate that this concept is applicable for remediation of various sources of water contaminated with both short- and long-chain PFAAs.

Keywords:

Electrosorption; PFOA; PFBA; Regeneration of activated carbon; Activated carbon felt; Surface chemistry.

1- Introduction

Remediation of water contaminated with perfluoroalkyl acids (PFAAs) as persistent organic pollutants is extremely challenging [1, 2]. Fixed-bed adsorption by granular activated carbon (GAC) is currently the prevailing technology at large scale [2, 3]. However, perfluorocarboxylic and sulfonic acids, e.g. perfluorooctanoic acid (PFOA) and perfluorooctylsulfonic acid (PFOS), respectively, are a challenge even in activated carbon (AC) adsorption, as they are anionic (at all relevant pH conditions) and highly water-soluble [1-3]. The occurrence of shorter-chain PFAAs in water sources has resulted in serious problems, e.g. early breakthrough and/or no removal of perfluorobutanoic acid (PFBA) in AC filtration [3-5]. So far, on-site regeneration of AC adsorbers is not state of the art [2]. A recent review on the specific objectives in the removal of short- and long-chain PFAAs by adsorption addressed regeneration of PFAA exhausted adsorbents as one of the biggest challenges [2].

Adsorption coefficients (K_d) of PFAAs on various AC materials can differ up to 4 orders of magnitude for the same adsorbate [6-10]. This large variance was attributed to different abilities for providing electrostatic interactions and charge compensation provided by positively charged surface sites (anion exchange capacity, AEC) of AC [6, 8, 11]. These results implicate that the adsorption affinity of the ACs for PFAAs can be controlled by manipulating the balance of their surface charges. Thus, our aim was to investigate the application of external electrical potentials, known as electrosorption, for increasing the adsorption of PFAA anions and facilitating their facile regeneration by desorption.

Electrosorption of PFOA and PFOS on graphene- and carbon nanotube-based electrodes has been described in three previous publications [12-14]. Li et al. [12] reported that enhanced electrostatic attraction between PFOA or PFOS anions and a polarized carbon nanotube-based

electrode (+600 mV V vs. Ag/AgCl) leads to a 2-fold increase in maximum loadings (based on Langmuir isotherm fitting) compared with open circuit attempts. In these studies, various factors influencing the process, e.g., reversibility and long-term cyclability of the process and competitive adsorption of target pollutants with non-target compounds such as inorganic and organic ions have not been investigated. Such information is essential for practical application of electrosorption.

Kim et al. [15] recently reported promising results in controlling adsorption of PFAAs on electrodes coated with redox co-polymers with sub-units of 2,2,6,6-tetramethylpiperidin-1-oxyl and 2,2,6,6-tetramethylpiperidine. In this case a 5-fold increase in adsorption capacity of PFOA was observed when the applied potential was varied between -1000 mV and $+1000$ mV vs. Ag/AgCl. In all these studies, synthesized and self-fabricated electrodes were applied. Electrosorption of PFAAs on commercial AC materials has not been studied yet. Nevertheless, AC materials are the most widely applied electrode material in the fast developing field of capacitive deionization (CDI), i.e. removal of inorganic ions by electrosorption/desorption, with pilot and full-size applications [16, 17]. Attrition of the AC electrodes by direct and/or indirect oxidation and reduction under electrical potentials has been posed as a serious drawback for achieving a stable performance of the process over prolonged polarization times [18-20]. In fact, it is well-known that the changes in AC properties induced by anodic and cathodic potentials may lead to performance decline of CDI cells [21-24]. Applying milder potentials on the electrodes resulted in more stable performance [25, 26]. Thus, our intention was to mitigate carbon attrition by a proper material selection allowing charge-reversal already at mild positive or negative potentials. In this respect, the potential of zero charge (E_{PZC}) of the AC electrodes was considered as important selection criterion – a strategy that has not been applied yet in electrosorption of organic compounds.

Prospectively, electrosorption could be used as pre-concentration step in combination with subsequent degradation processes. In general, due to the recalcitrance of PFAAs practically all degradation processes require harsh conditions and/or long reaction times and as such are not applicable for treatment of large volumes or flows of contaminated water with trace levels of PFAA contamination [1, 27]. Consequently, a combination of membrane filtration and electrochemical oxidation of PFAAs in the concentrated retentate was recently proposed as a pre-concentration-degradation strategy [28]. Another promising pre-concentration approach could be an electro-stimulated adsorption, i.e. treating the large volume of incoming water (V_{ads}) containing PFAAs by favorable electroadsorption conditions and providing a low-volume concentrate (V_{des}) by electrodesorption of PFAAs from the saturated adsorbent electrodes. Reaching a low $V_{\text{des}}/V_{\text{ads}}$ ratio or a high concentration factor is the goal of this approach.

In this study we show for the first time that by applying electrical potentials to conductive commercial activated carbon felts (ACFs), ad- and desorption of PFOA and PFBA can be effectively controlled. Thanks to their easy handling, high mechanical integrity, electrical conductivity, regeneration potential and very high surface area, ACFs have numerous advantages compared to AC powders or granules [18, 29]. These materials are specifically attractive in electrochemical applications because they do not require particular shaping and can be used directly as free-standing electrodes [18, 30]. A growing number of studies for potential novel applications of ACFs was published in the last years, involving commercial materials in most cases [29]. In addition, ACFs enjoy very high adsorption affinities toward PFAAs [8, 11, 31]. Based on adsorption isotherm data for PFAAs at positively and negatively charged ACFs, we provide a first estimation of the concentration factor that is achievable in a fixed-bed

electrosorption unit. Special emphasis was placed on the mitigation of performance decline of an electrosorption cell over prolonged polarization times (10 electroadsorption/-desorption cycles).

2. Materials and Methods

2.1. Materials

PFOA and PFBA were purchased from Sigma-Aldrich (USA) with 96% and 98% purity, respectively. HCl (fuming 37%), NaOH, NaHCO₃, KCl, NaNO₃, MgSO₄, CH₃COONH₄, Na₂CO₃ and Na₂SO₄ (all in highest available purity) were obtained from Merck (Germany). Methanol (99.9%) was purchased from CHEMSOLUTE (Germany). Suwannee River natural organic matter (SRNOM, reference number: 2R101N) was obtained from the International Humic Substances Society (IHSS).

2.2. Textural and chemical surface properties of activated carbon felts

The ACFs were purchased from Jacobi CARBONS, Sweden. The commercial names of these ACFs are ACTITEX FC 1501 (ACF1 in this study), ACTITEX FC 1001 (ACF2) and ACTITEX WK L20 (ACF3). According to the company information, these ACFs are all made from synthetic rayon-based viscose fiber as precursor. In addition, a defunctionalised carbon felt (DeACF3, defunctionalised ACF3) was prepared by thermal treatment in N₂/H₂ atmosphere. In brief, a certain amount of ACF was placed in a tube furnace, purged with nitrogen for 1 h and then with hydrogen for 30 min at ambient temperature, heated up with a ramp of 50 K/min up to 900 °C and kept at 900 °C for 2 h. Finally, the sample cooled down to ambient temperature under a flow of hydrogen. Detailed description of the characterisation procedures can be found in a previous study [32] (note that CACF in [32] = ACF3 in the present study). The most important

characterisation data are shown in Tables S1 and S2 in Supporting Information. Prior to use, the ACFs were washed first with methanol and then rinsed 5 times with deionized water. Finally, the ACFs were dried at 80 °C on air and kept in a desiccator for further use.

2.3. Electrochemical characterisation of activated carbon felts

Cyclic voltammetry (CV) experiments were carried out in three-electrode cells at room temperature, using commercial Ag/AgCl reference electrodes (REs, Sensortechnik Meinsberg SE11, Germany) and platinum plates (1 cm × 4 cm) as counter electrode (CE) in 1 M Na₂SO₄ solution. Before and after each measurement, the potential readings of the REs were verified by comparison to fresh ones. The variation was within the range of 10 mV. The electrochemical cells were made of glassware. A high resolution potentiostat/galvanostat (MSX-8, ScioSpec, Germany) was used for performing measurements of CV and electroadsorption/-desorption experiments.

Electrochemical impedance spectroscopy (EIS) measurements were applied to identify relevant frequency ranges for investigating the capacitance minimum. EIS was measured from 3 mHz to 1 kHz with various potentials (from +500 mV to -500 mV) by means of a potentiostat/galvanostat/impedancemeter (OGS100, OrigaLys, France). EIS was carried out in custom-made two-piston cells that enabled testing in a three electrode setup. Contacting of the current collectors was accomplished by titanium pistons. A piece of ACF was introduced from side to the cell and served as quasi reference electrode. It was separated from other electrodes by means of a glass-fiber separator (type GF/D, Whatman, GE healthcare life science). The reference potential of the quasi reference electrode was determined versus the commercial Ag/AgCl RE. The results were reported based on the potential of Ag/AgCl RE. Electrolyte filling was accomplished by inserting the electrolyte via filling tubes and applying a small negative pressure to ensure

complete filling [33]. A schematic drawing of the cell is shown in Figure 1S in Supporting Information. For more details on the cell, we refer the readers to [33]. Open circuit potentials (E_0) of the ACFs were also measured by means of the OGS100 instrument at pH 7.

Differential capacitance measurements were carried out in order to recognize E_{PZC} from the capacitance minimum [34]. The frequencies at which the imaginary part of Z became nearly independent of the frequency were monitored by means of Nyquist plots. These frequencies were used to calculate the capacitance C from the imaginary part (Z_{Im}) of the impedance using Eq. 1:

$$C = - (\omega Z_{Im})^{-1} \quad (1)$$

where ω is the angular frequency ($\omega = 2\pi/\text{period}$).

2.4. Analytical methods

Analysis of PFOA and PFBA was carried out by means of a liquid chromatography system coupled to a single-stage quadrupole mass spectrometer with electrospray ionization (LCMS-2020; SHIMADZU Corporation, Japan). The analytical procedure was discussed elsewhere in detail [6]. For concentrations in the range 1 $\mu\text{g/L}$ - 1 mg/L the correlation coefficients (R^2) of the linear calibration curves for PFOA and PFBA were > 0.99 . The standard deviation of single values (estimated from 5 parallel measurements) was around 5%. The detection limits for PFAAs were about 0.05 $\mu\text{g/L}$.

2.5. Electrosorption experiments

As mentioned earlier, all electroadsorption/-desorption experiments were carried out in a series of batch three-electrode cells (100 mL vessels containing around 70 mL electrolyte) connected to a potentiostat. In these cells, ACF was used as working electrode (WE), a commercial

Ag/AgCl electrode as RE, and platinum plate (1 cm × 4 cm) as CE. Na₂SO₄ solutions (10 mM if not stated otherwise) were used as electrolyte which was stirred by a magnetic stirrer. Figure 2S shows a scheme of the three-electrode cell. The pH of the system was adjusted to the desired values by adding 0.1 M HCl or NaOH solution. After adjusting pH, certain concentrations of the target solutes were spiked from stock solutions. In electrodesorption experiments, after reaching equilibrium in electrosorption, the potential was converted to respective values.

The amount of PFOA and PFBA adsorbed by the ACFs (adsorbate loading) was calculated from Eq. 2:

$$q_e = \frac{V \times (C_0 - C_e)}{m} \quad (2)$$

here q_e (mg/g) denotes loading of adsorbate on the adsorbent at equilibrium. The initial adsorbate concentration and its concentration in solution at equilibrium are addressed by C_0 and C_e (mg/L), respectively. V (L) denotes the volume of solution and m (g) is the mass of the adsorbent or WE.

The single-point adsorption coefficient K_d (L/g) of the solutes on the adsorbents can be calculated by means of Eq. (3):

$$K_d = \frac{q_e}{C_e} \quad (3)$$

Equilibrium was considered to be approached after 2 d, as no significant changes in the aqueous phase solute concentrations were observed ($\leq 5\%$) at further prolonged contact times.

2.6. Theoretical approach

2.6.1. Electrosorption isotherms

The experimental data were fitted with a linearised form of the empirical Freundlich equation (Eq. 4):

$$\log q_e = n \times \log C_e + \log K_F \quad (4)$$

with K_F ((mg/g)/(mg/L)ⁿ) as the Freundlich constant which denotes the adsorption affinity, while n is the dimensionless Freundlich exponent.

2.6.2. Calculation of V_{des}/V_{ads} and concentration factor

Prospectively, the batch reactor should be replaced by a continuous flow system for many practical applications. In a fixed-bed flow through system the adsorbent bed is progressively loaded with the adsorbate from inflow to outflow reaching the equilibrium loading (q_{ads}) related to the inflow concentration (C_{in}) until breakthrough occurs. In a simplified approach, we assume a step-like breakthrough curve. Band-broadening effects due to incomplete establishment of adsorption equilibria or dispersion effects were neglected. A concentration factor $V_{des}/V_{ads} = 1/F$ can be calculated by Eq. 5 (for its derivation see Supporting Information):

$$\frac{V_{des}}{V_{ads}} = \frac{X_{des}}{\left(\frac{K_{F,ads}}{K_{F,des}}\right)^{\frac{1}{n}} - 1} \quad \text{with} \quad X_{des} = 1 - \frac{K_{F,des}}{K_{F,ads}} \quad (5)$$

where V_{ads} is the water volume cleaned in the adsorption step, V_{des} denotes the volume of water which is needed for desorption, $K_{F,ads}$ and $K_{F,des}$ are Freundlich coefficients in adsorption and desorption steps, respectively, and n is the Freundlich exponent. Eq. 5 is based on the scenario that the contaminated influent water is used as eluent in the desorption step. This explains a limited value of the achievable extent of desorption $X_{des} < 1$. Please note that Eq. 5 is applicable if the Freundlich exponents in adsorption (n_{ads}) and desorption (n_{des}) are similar, i.e. $n_{ads} \approx n_{des} \approx n$. If $n_{ads} \neq n_{des}$, Eq. S6 (Supporting Information) has to be used for calculating the concentration factor.

3. Results and discussion

3.1. Characterisation of the ACFs

3.1.1. Textural and chemical surface characteristics

ACFs differ significantly in their pore size distributions (PSD) from common ACs (Figure 3Sa). The ACFs investigated here are mostly microporous (Figure 3Sb) with differences in total pore volume and surface area (see Table 1S in Supporting Information). In fact, ACF1 has the highest surface area ($1600 \text{ m}^2/\text{g}$) and total pore volume ($0.74 \text{ cm}^3/\text{g}$), followed by ACF2, ACF3 and DeACF3. Table 2S in Supporting Information lists chemical characteristics of the surface groups of the ACFs. ACF3 has the highest concentration of acidic groups, which were largely eliminated by thermal treatment in N_2/H_2 atmosphere resulting in DeACF3. Furthermore, DeACF3 contains the highest anion exchange capacity ($\text{AEC} = 0.2 \text{ } \mu\text{mol}/\text{m}^2$) at pH 7, followed by ACF1, ACF2 and ACF3. The opposite order is true for cation exchange capacities (CECs). The thermal treatment also eliminated the oxygen content of ACF3 from 13.7 wt% to 1.1 wt% in DeACF3, while oxygen contents of ACF1 and ACF2 are 15.9 wt% and 3.9 wt%, respectively. Nitrogen contents of all ACFs are less than 1 wt%.

3.1.2. Electrochemical characterisation

Figure 1a illustrates Nyquist plots at +100 mV obtained in 1 M Na_2SO_4 solution at pH 7. These results suggest a characteristic frequency of 71 mHz for all ACFs above which the imaginary part of Z becomes nearly independent of the frequency. This value was considered as the upper limit of frequency for measuring the differential capacitance as described below.

Capacitance values for the ACFs were calculated using Eq. 1 at frequencies of 3.1, 7.9, 16 and 71 mHz between -500 mV and +500 mV. Figure 1b shows differential capacitance curves

measured at a frequency of 3.1 mHz versus potential, while the differential capacitance curves obtained at other frequencies are shown in Figure 4S. The capacitance values were normalized to the specific surface areas of the ACFs. The minimum capacitance value is considered as E_{PZC} of the respective ACF [34]. Thus, E_{PZC} values for ACF1, ACF2, ACF3 and DeACF3 are around +75, +200, +300 and -150 mV, respectively.

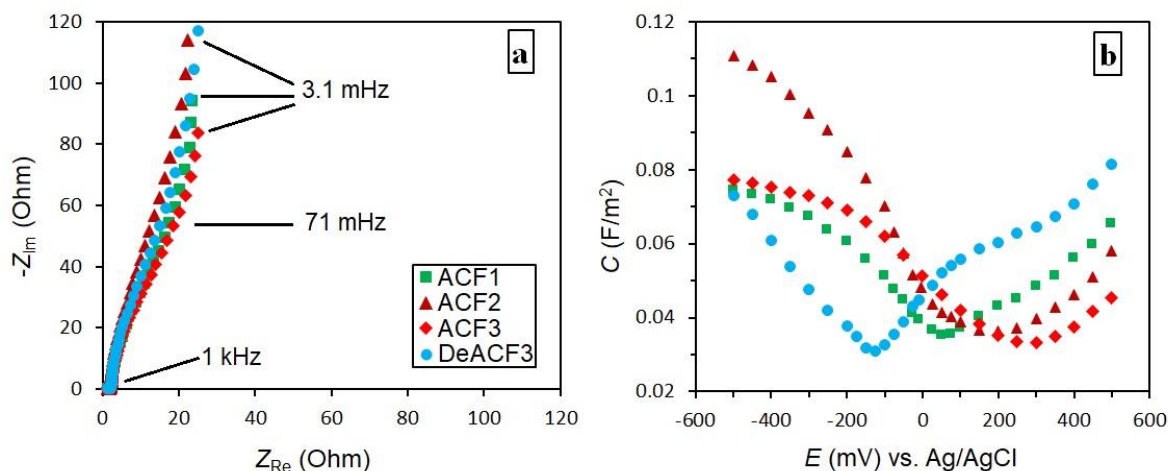


Figure 1. Nyquist plots of the negative imaginary part of the impedance ($-Z_{im}$) versus the real part (Z_{Re}) measured for the ACF electrodes at +100 mV in 1 M Na_2SO_4 (a). Differential capacitance (C) of the ACFs at frequency 3.1 mHz versus the potential (b). Electrolyte was 1 M Na_2SO_4 solution at pH 7. The capacitance was normalized to specific surface areas of the ACFs. The minimum capacitance values are considered as E_{PZC} .

As can be seen in Figure 1b, when an applied potential crosses the E_{PZC} towards more positive (or more negative) potentials, anion-adsorption (or cation-adsorption) is enhanced correspondingly [25, 35]. A low absolute E_{PZC} value of a carbon electrode allows easy charge reversal by applying mild potentials, thus lowering carbon electrode erosion and improving long-term performance. As a consequence, DeACF3 and ACF1 were considered as more appropriate than ACF2 and ACF3 for the intended electroadsorption/-desorption approach.

The E_{PZC} values of the ACFs were measured under similar conditions and at pH 7. Differential capacitances in Figure 1b were normalized to the surface areas of the ACFs. Therefore, the differences in E_{PZC} of the various ACFs can be attributed to their chemical surface properties. Figure 2 shows the effect of chemical surface properties of the ACFs on E_{PZC} . The order in E_{PZC} (ACF3 > ACF2 > ACF1 > DeACF3) is opposite to the order of pH_{PZC} of the ACFs (Figure 2a). For example, $pH_{PZC} = 5.9$ for ACF3 means that at circumneutral pH the net charge on the surface of ACF3 without any applied electrical potential is negative. Therefore, the applied positive potential firstly needs to compensate the negative charge associated to functional surface groups until a balanced net charge is reached at E_{PZC} (around +300 mV).

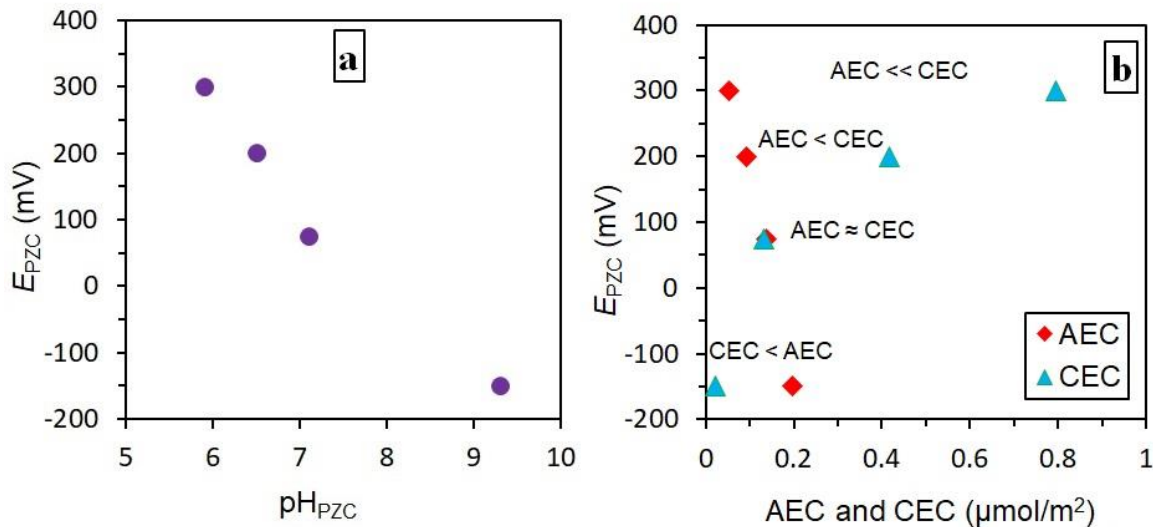


Figure 2. Effect of surface chemical properties of the ACFs on E_{PZC} . AEC, CEC and E_{PZC} were determined at pH 7.

While the applied positive potential crosses E_{PZC} ACF3 is finally positively charged. ACF1 with pH_{PZC} close to 7, i.e. with almost balanced surface net charge at pH 7 without potential, consequently has a lower E_{PZC} value (+ 75 mV), while DeACF3 with $pH_{PZC} = 9.3$ even has an E_{PZC} (-150 mV) in the negative potential range. As can be seen in Figure 2b, when $CEC > AEC$, namely in case of ACF2 and ACF3, the E_{PZC} locates in the positive potential range. However, when CEC

< AEC e.g. in case of DeACF3 the E_{PZC} is in the negative range, although ACF1 with $CEC \approx AEC$ has the lowest E_{PZC} absolute value. Note that AEC and CEC as anion and cation exchange capacity of the carbon are related to the density of positively and negatively charged surface functional groups at pH 7 (without external potential).

The study on cyclic voltammograms (CVs) of the ACFs showed quasi-rectangular curve shapes for all ACFs at the scan rate of 1 mV/s in accordance with their capacitive behaviour. Figure 3 compares capacitance values of the ACFs obtained from CVs at a scan rate of 1 mV/s with those calculated by means of EIS at a frequency of 3.1 mHz. First of all, the capacitance values obtained from both EIS and CVs are comparable. Both, EIS and CV experiments were performed in 1 M Na_2SO_4 solutions at pH 7. Therefore, the capacitance is associated to adsorption of anions (SO_4^{2-}) on the positively charged ACFs ($E > E_{PZC}$). On the other hand, adsorption of cations (Na^+) results in capacitance of the ACFs polarized with $E < E_{PZC}$. It can be seen from Figure 3 (EIS curves) that ACF2 has the highest total capacitance.

In fact, by polarization of ACF2 to -500 mV or +500 mV, its capacitance reaches to around 0.12 F/m² and 0.06 F/m², respectively, resulting in a total capacitance of 0.18 F/m². ACF3 shows also a higher capacitance coming from adsorption of cations (for $E < E_{PZC} = +300$) than from anions (for $E > E_{PZC} = +300$). In contrast, ACF1 and DeACF3 have total capacitance values around 0.16 F/m² with approximately equal contributions from adsorption of cations and anions. These results confirm our conclusion on selection of ACF1 and DeACF3 for electrosorption of PFAA anions. Nevertheless, ACF2 and ACF3 seem to be good candidates for electrosorption of organic cations. The cyclic voltammograms recorded at various scan rates can be found in Figure 5S in Supporting Information.

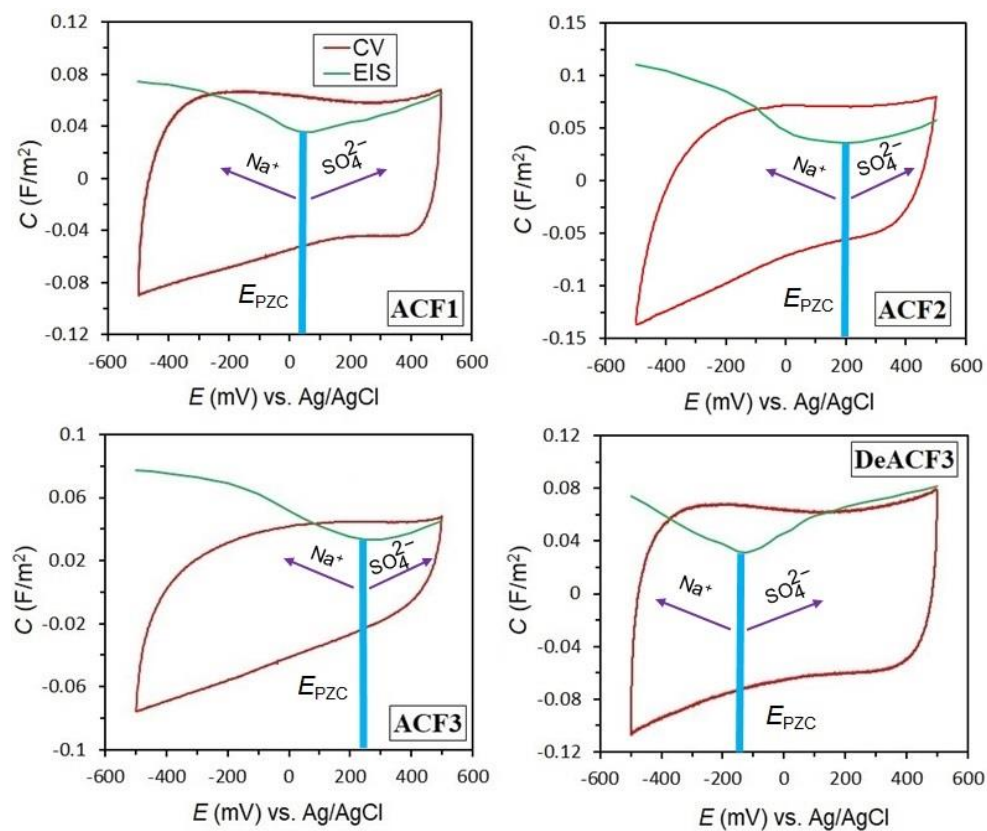


Figure 3. A comparison between capacitance values obtained from CV at scan rate 1 mV/s and EIS at frequency 3.1 mHz. The experiments were performed in 1 M Na₂SO₄ at pH 7.

3.2. Electroadsorption/-desorption experiments

3.2.1. Potential dependence and electroadsorption mechanism

ACF1 and DeACF3 were applied for electroadsorption experiments. Figure 6Sa in Supporting Information shows the kinetics of adsorption and electroadsorption (at +500 mV) of PFOA on ACF1. Equilibrium was approached within less than 48 h as no significant changes in aqueous phase solute concentrations were observed ($\leq 5\%$) at further prolonged contact time. However, around 90% of total loading is achieved already during the first 3 hours of the process. Figure 6Sb shows the kinetics data fitted with the pseudo-second-order kinetics equation (Eq. S9 in Supporting Information). The calculated pseudo-second-order rate constants for adsorption and

electroadsorption are nearly identical ($k_2 = (0.147 \pm 0.008)$ g/mg/h). This means no significant effect of potential on adsorption kinetics was observed.

Figure 4a shows adsorption coefficients (K_d) in electrosorption of PFOA on ACF1 versus potentials. It is worth pointing out that the PFAAs are chemically stable on carbon electrodes in a wide potential range (-1000 mV to 1000 mV [12-14]). The plot of K_d (at pH 6-7) versus potential results in a bell-shaped curve with a maximum at +500 mV with respective K_d values up to 10^6 L/kg. This K_d value is about 44 times higher than the values at negative potentials. Note that the presented K_d values were measured with the same initial solute concentrations ($C_0 = 1$ mg/L) but approaching different equilibrium states. Adsorbent loadings with PFOA range from 9 to 24 mg/g. As E_{PZC} and E_0 of AFC1 are +75 mV and +225 mV, respectively, at potentials $> +75$ mV the net charge on ACF1 is positive. Therefore, the enhancement in K_d at potentials $> +75$ mV is most likely due to electrostatic attraction.

Interestingly, increasing the potential further to +700 mV, +850 mV and +1000 mV decreases the adsorption of PFOA significantly. The reason for this counterintuitive behavior is that applying electrical potentials on the AC electrode enhances also the polarity of the surface. This affects also the hydrophobic interactions between the fluorinated tail of PFOA and the carbon surface [6]. Thus, an increasingly charged surface can have a negative effect on adsorption of PFOA as the competition by water molecules becomes more dominant [36]. Moreover, a decrease in K_d value could be caused by changing the chemical properties of the ACF from direct and indirect oxidation under positive potentials [18, 19]. These effects on chemical surface properties and electrosorption performances of the ACFs will be discussed in section 3.2.5. On the other hand, applying potentials more negative than the E_{PZC} (+75 mV) of ACF1 decreases significantly

the adsorption affinity of PFOA. This is probably caused by electrostatic repulsion between negatively charged sites of ACF1 and PFOA as carboxylate.

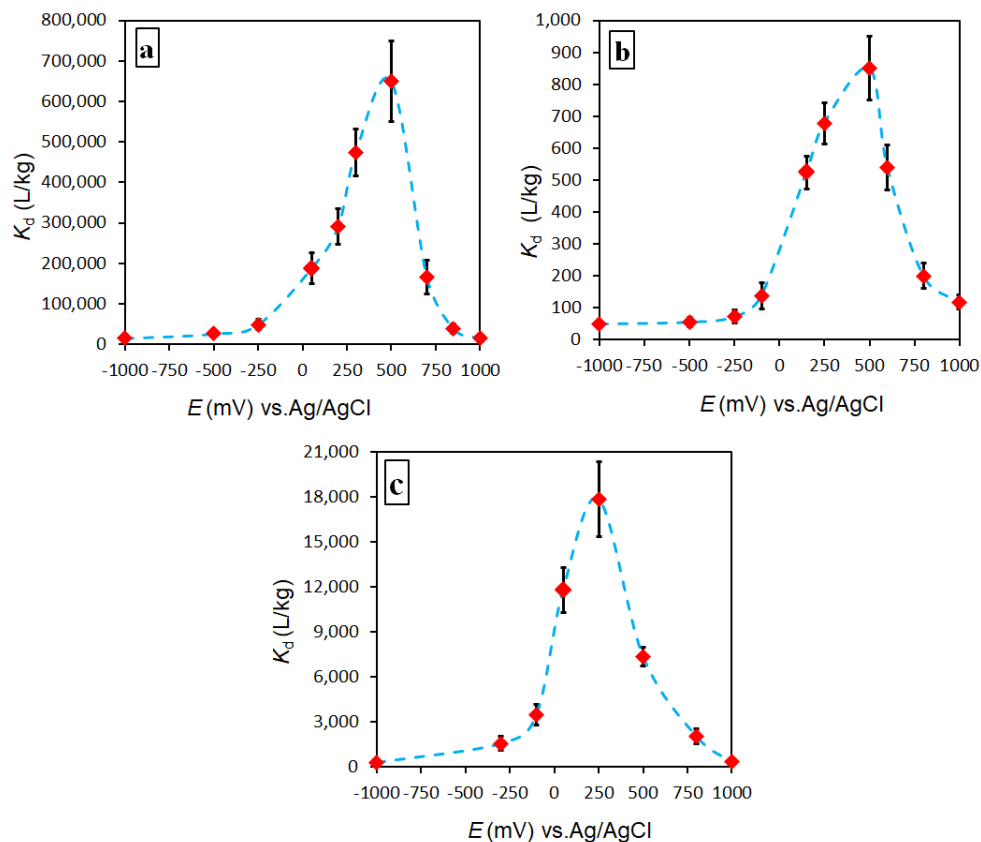


Figure 4. Effect of electrical potential on electroadsorption of PFOA on ACF1 (0.04 g/L) (a) PFBA on ACF1 (1.5 g/L) (b) and PFBA on DeACF3 (0.33 g/L) (c). Experimental conditions: $C_0 = 1$ mg/L PFOA or PFBA; electrolyte: 10 mM Na_2SO_4 at pH 6-7; duration of each individual experiment: 2 days. The error bars are standard deviations of 4 individual experiments. In plot (c) adsorption experiments at ± 1000 mV showed insignificant depletion of the analytes $C_e/C_0 \geq 0.95$. The corresponding reported K_d values ($K_d = 160$ L/kg) were then approximated based on a 5% depletion and thus are upper limits of true K_d .

Figures 4b and c show K_d values in electroadsorption of PFBA on the two felts versus potential. Similar to PFOA, bell-shaped curves were obtained with PFBA as well. The potentials for maximum adsorption coefficients of PFBA are different on DeACF3 and ACF1, i.e. +250 mV

versus +500 mV, respectively. The reason is probably the lower E_{PZC} (-150 mV) of DeACF3 compared with E_{PZC} (+75 mV) of ACF1. In the absence of externally applied potentials, DeACF3 bears already a positive net charge at circumneutral pH due to the prevalence of basic surface groups ($pH_{PZC} = 9.3$). ACF1 ($pH_{PZC} = 7.1$) has an equal density of positive and negative charges under these conditions. Applying positive electrical potentials improves adsorption of PFOA and PFBA anions in both cases but obviously the optimum charge density is reached at lower potential absolute values for DeACF3 which already bears positive charges related to its functional groups. At the same time, shifting electrical potential to more negative values firstly has to compensate these charges on DeACF3 so that there is a shift in the declining branch of the K_d curve towards lower potentials. These results yield a general message for applying electrosorption for removal of ionized organic pollutants: surface functional and electrochemical properties of AC electrodes together must be considered for optimal design of the process.

The general finding that sorption of anionic and cationic organic compounds increases or decreases by applying positive or negative potentials, respectively, was reported in previous studies [37-41]. Our data on electrosorption of PFOA and PFBA indicate that PFAAs anions are specifically sensitive towards the charging state of the carbon surface as large differences in K_d depending on applied potential were observed (two orders of magnitude variation for PFBA compared to less than one order reported for various organic anions and cations [37-41]). Furthermore, the formation of bell-shaped curves from plotting electrosorption parameters of PFOA and PFBA versus potentials observed in the present study are in agreement with predictions of Fischer [36] for electrosorption of organic ionic and nonionic compounds. In the quantitative model developed by this author, adsorption on a charged electrode is considered to be equivalent to the moving of a slab of dielectric (organic adsorbate or water) in a parallel plate capacitor formed

by the charged solid surface and the outer Helmholtz plane layer of counterions. Based on this model, increasing the applied potential will increase the force pulling water inside and pushing out the pollutant (i.e. favoring adsorption of water over organic pollutant). This results in bell-shaped curves of electrosorption K_d values over applied potential with the position of the maximum shifting to the positive or negative potential range depending on the charge of the adsorbing pollutant molecule [36]. Another plausible image for explaining the decrease in K_d values is the following: high electrical potentials make the carbon surface more polar, i.e. more hydrophilic. This favors adsorption of water over organic adsorbates. To our knowledge, such an electrosorption behaviour of organic compounds have been rarely discussed in literature. The reasons as well as a detailed discussion on potential dependence in electrosorption of organic compounds can be found in Supporting Information.

3.2.2. Electrosorption isotherms and concentration factor

Figure 5a shows electrosorption isotherms of PFOA on ACF1 polarized at +500 mV, -100 mV, and -1000 mV and compares these results with adsorption (no potential) isotherms. A significant effect of electrical potentials on the adsorption isotherms is obvious. The experimental data were fitted with a linearized form of the Freundlich equation (Figure 5b). Note that the Freundlich equation can only be applied within a certain solute concentration range, i.e. significantly below the maximum loadings. Table 1 lists the isotherm parameters. Table 3S shows a comparison between adsorption and electroadsorption of PFOA on ACF1 with results from adsorption of PFOA on some other adsorbents, which were very recently published. It can be seen that the single-point adsorption coefficient of PFOA ($K_d = 8.3 \times 10^5$ L/kg calculated at $C_e = 20$

$\mu\text{g/L}$) in electroadsorption at +500 mV is in the upper range of K_d values calculated for these adsorbents at comparable C_e of PFOA.

Freundlich isotherm parameters in adsorption and electroadsorption of PFOA on ACF1 are listed in Table 1. As discussed earlier, when Freundlich exponent parameters (n) are similar in electroadsorption and electrodesorption, Eq. 5 can be applied to calculate the volume of water (V_{des}) needed for deloading of the adsorbent. It can be seen in Table 1 that Freundlich exponent parameters for electroadsorption at +500 mV (n_{ads}) and at negative potentials (n_{des}) are similar. Therefore, the simplified Eq. 5 is applied to calculate the volume ratio of water needed for desorption related to treated water which is the reciprocal of the concentration factor ($V_{\text{des}}/V_{\text{ads}})_{+500/-1000} = 1/F_{+500/-1000}$ for electroadsorption at +500 mV and electrodesorption at -1000 mV:

$$\frac{V_{\text{des}}}{V_{\text{ads}}} = \frac{0.95}{\left(\frac{200}{9.8}\right)^{\frac{1}{0.64}} - 1} = 0.0087 \quad \text{with} \quad X_{\text{des}} = 1 - \frac{9.8}{200} = 0.95$$

In words, by means of potential-controlled adsorption and desorption 95% of adsorbed PFOA can be released in an aqueous concentrate of about 0.9% of the treated water volume resulting in a concentration factor of $F_{+500/-1000} = 115$. Similarly, changing the electrodesorption potential to -100 mV yields $F_{+500/-100} = 71$, while $F_{\text{no potential}/-100} = 41$ if adsorption is performed without applied external potential.

The concentration factors from electroadsorption can be compared with concentration factors in other separation processes, e.g., reverse osmosis. In USA, two treatment plants for PFAAs-contaminated water use reverse osmosis with polyamide Hydranautics ESPA2 membranes in a three stage array with a water flux of 12 gfd (gallons per square foot per day) receiving 85%

recovery (cleaned water) [42], i.e. at a concentration factor of 6.7. The concentration factors calculated in the present study based on equilibrium data from batch experiments are at least by a factor of 10 higher which illustrates the potential of the electrosorption method. Clearly, technically achievable concentration factors under application conditions can be lower and have to be determined in site-specific studies.

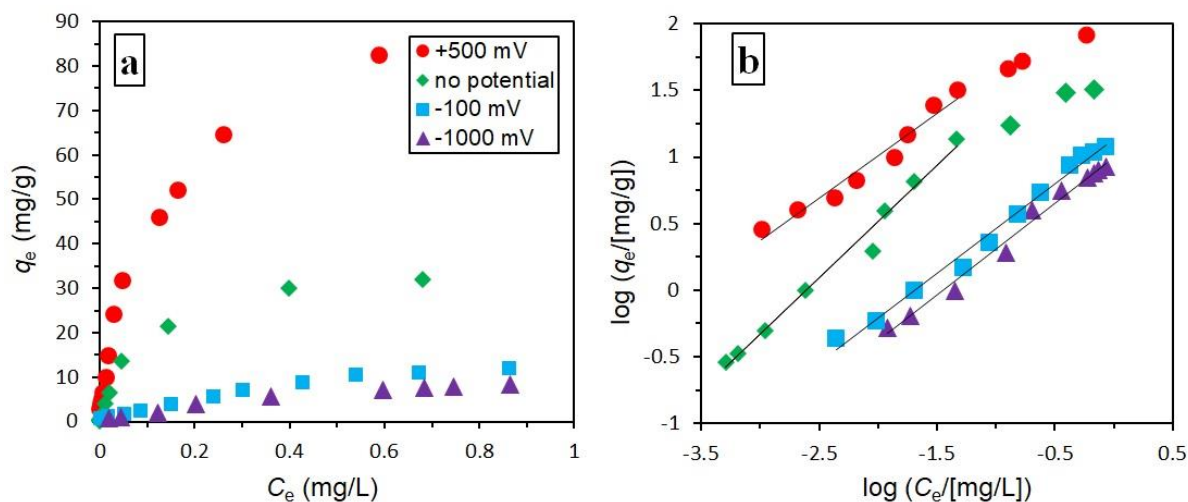


Figure 5. Experimental data (a) from electrosorption at +500 mV, -100 mV and -1000 mV (vs. Ag/AgCl) and adsorption (no potential) isotherms of PFOA on ACF1 fitted with Freundlich equation (b). Experimental conditions: $C_{0, \text{PFOA}} = 1 \text{ mg/L}$; electrolyte: 10 mM Na_2SO_4 at pH 6-7; equilibration time in each individual experiment: 2 days.

Table 1. Freundlich parameters for electrosorption and adsorption without external potential of PFOA on ACF1.

Experiment	Potential ^a (mV)	Log ($K_F/[(\text{mg/g})/(\text{mg/L})^n]$)	n	R^2
PFOA on ACF1	No potential	2.20	0.84	0.985
PFOA on ACF1	+500	2.30	0.64	0.963
PFOA on ACF1	-100	1.13	0.67	0.989
PFOA on ACF1	-1000	0.99	0.69	0.987

^a versus Ag/AgCl as reference electrode.

3.2.3. Effect of electrolyte pH

In Figure 6, the pH-driven effects on adsorption of PFOA (no external potential) are compared with the potential-driven effects. The effects are as expected: charging ACF1 ($\text{pH}_{\text{PZC}} = 7.1$) positively by both, decreasing pH from 7 to 3 or applying a positive potential (+500 mV at pH 7), increases adsorption affinity (K_d) of PFOA. Charging ACF1 negatively by increasing pH to 9 or applying a negative potential (-1000 mV) decreases adsorption coefficients.

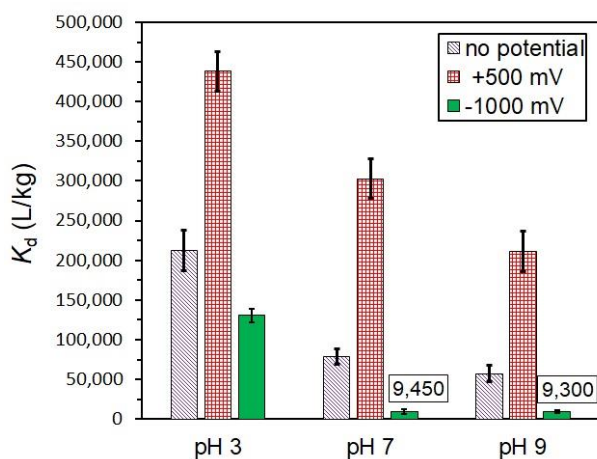


Figure 6. Effect of electrolyte pH on electrosorption of PFOA on ACF1 (16 mg/L). Experimental conditions: $C_0 = 1$ mg/L in 10 mM Na_2SO_4 ; equilibration time in each individual experiment: 2 days. The error bars are standard deviations from 4 individual experiments. The potentials are versus Ag/AgCl.

It is evident from Figure 6 that the external electrical potential at circumneutral pH has a stronger effect on the adsorption behaviour (about factor 30) than changing the pH (a factor of 4 with no external potential). This is in agreement with what observed by Ban et al. [38] in electrosorption of naphthoic acid and naphthalenesulfonic acid anions at different electrode potentials and electrolyte pH values on AC. Another message from these results is that even at pH = 3 or 9, i.e. under conditions of prevailing positive or negative chemical surfaces charges, respectively, PFOA

adsorption can be manipulated by applying external electrical potentials. Nevertheless, the strongest effect of electrical potential is observed at pH 7 where the chemical surface charges resulting from protonation/deprotonation equilibria are balanced and E_{PZC} has a low positive value.

In contrast, Niu et al. [14] found enhanced PFOA electrosorption at a positively polarized carbon nanotube-graphene composite electrode when pH was raised from 3 to 9. This behavior is counterintuitive since PFOA must be expected to be nearly completely in the anionic state over the whole considered pH range ($pK_a = 0-1$ [43]) and the deprotonation of the carbon surface should increase electrostatic repulsion. Our results also don't confirm this observation as shown in Figure 6. Nevertheless, there remains uncertainty whether the pH in the confined carbon pores could deviate from the measurable bulk pH so that pH effects on PFOA speciation close to adsorption sites might still occur depending on the type of carbon material applied.

3.2.4. Effects of inorganic ions and dissolved natural organic matter

It has been reported that coexisting inorganic anions and cations can affect adsorption of PFAAs on various adsorbents [3, 44]. However, their effects on electrosorption has not been studied yet. Figure 7 shows electroadsorption and subsequent electrodesorption of PFOA and PFBA by switching potential from +500 mV (+250 mV in case of PFBA on DeACF3) to -1000 mV in the presence of different concentrations of Na_2SO_4 . Due to its divalent charge, sulfate can be expected a stronger competitor for electrostatic interactions than a monovalent anion like e.g. chloride. An increase in Na_2SO_4 concentration from 10 mM to 200 mM reduces K_d values in electroadsorption of both PFOA and PFBA, however, by a factor less than 2 only. Negative potential has a strong repulsive effect on the adsorbed PFAAs even in presence of 200 mM Na_2SO_4 , leading to a 17-fold lower K_d at -1000 mV compared to +500 mV for PFOA and 70-fold

lower for PFBA on DeACF3. This indicates that the electroadsorption/-desorption concept for PFAAs is applicable for water containing even high concentrations of inorganic ions.

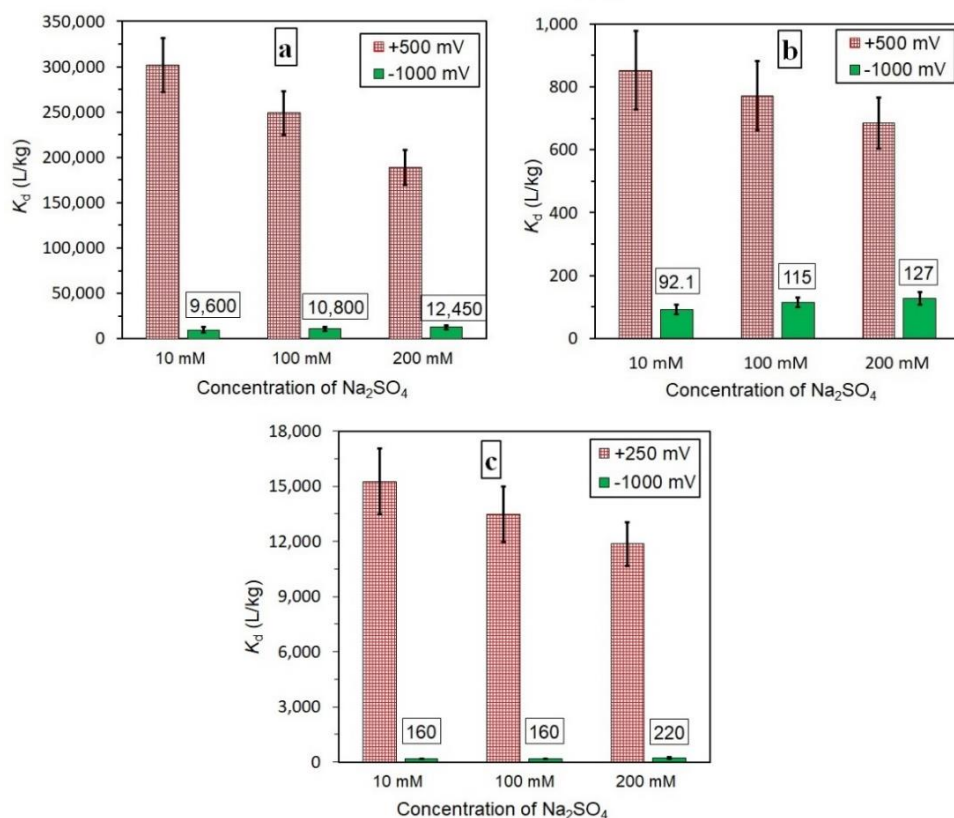


Figure 7. Effect of inorganic ions on electroadsorption/-desorption of PFOA and PFBA. a) PFOA on ACF1 (16 mg/L), b) PFBA on ACF1 (1.5 g/L) and c) PFBA on DeACF3 (0.33 g/L). Experimental conditions: $C_0 = 1$ mg/L PFOA or PFBA in x mM Na_2SO_4 at pH = 7; equilibration time in each individual experiment: 2 days. The error bars are standard deviations from 4 individual experiments. In plot c, the experiments at -1000 mV in 10 and 100 mM Na_2SO_4 showed insignificant depletion of the analytes $C_e/C_0 \geq 0.95$. The corresponding reported K_d values ($K_d = 160$ L/kg) were then approximated based on a 5% depletion and thus are upper limits of true K_d . The potentials are versus Ag/AgCl.

Dissolved natural organic matter (DNOM) often plays a competitive role in the adsorption process of organic compounds [45, 46]. The effect of DNOM on electroadsorption of PFAAs has not

been studied yet. Figure 8 shows electrosorption results for PFOA and PFBA in water containing 5 mg/L DNOM at pH 7.

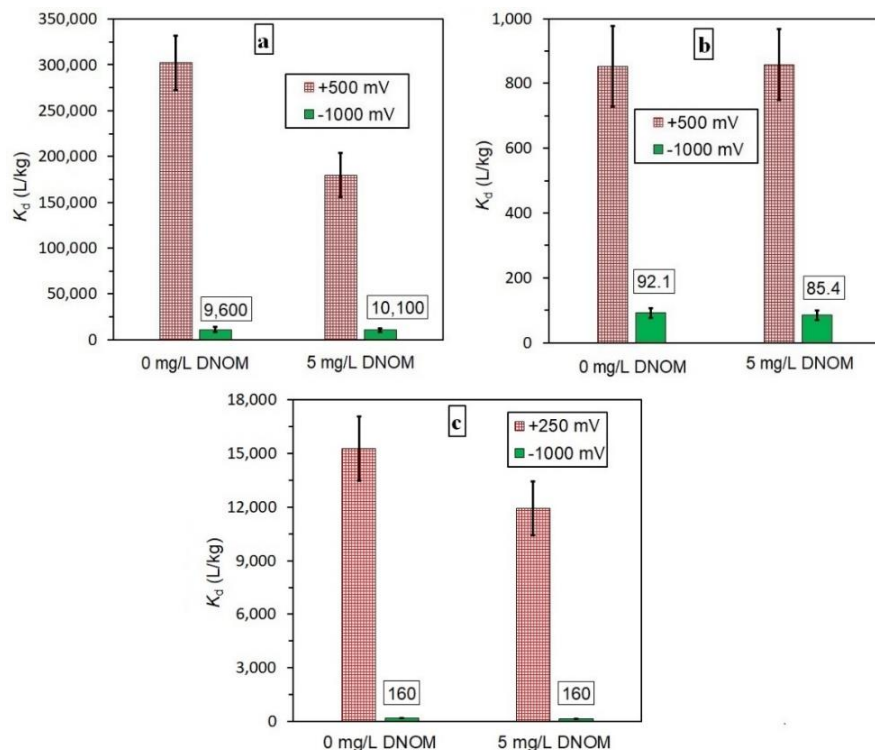


Figure 8. Effect of DNOM on electrosorption/-desorption of PFOA and PFBA. a) PFOA on ACF1 (16 mg/L), b) PFBA on ACF1 (1.5 g/L) and c) PFBA on DeACF3 (0.33 g/L). Experimental conditions: $C_0 = 1$ mg/L PFOA or PFBA in 10 mM Na_2SO_4 at $\text{pH} = 7$; equilibration time in each individual experiment: 2 days. The error bars are standard deviations from 4 individual experiments. In plot c, the experiments at -1000 mV showed insignificant depletion of the analytes $c/c_0 \geq 0.95$. The corresponding reported K_d values ($K_d = 160$ L/kg) were then approximated based on a 5% depletion and thus are upper limits of true K_d . The potentials are versus Ag/AgCl.

The presence of DNOM in solution reduces electroadsorption of the PFAAs only moderately by a factor < 2 . This effect is probably caused by competition between deprotonated DNOM molecules and the PFAA anions. Nevertheless, there is still a large difference between K_d values under electroadsorption and electrodesorption conditions, e.g. 18-fold in case of PFOA and 75-fold in

case of PFBA on DeACF3. Due to the very low concentrations of PFAAs in real contaminated waters ($\leq 1 \mu\text{g/L}$) the electrosorption data presented in this study ($C_{\text{PFOA}} \approx 100 \mu\text{g/L}$) are an approach to rather than a 1:1 image of real conditions.

3.2.5. Long-term electrosorption/-desorption experiments

In order to study the performance decline of the electrosorption cell over prolonged period of time, we first run 5 cycles of electrosorption of PFOA on ACF1 at +500 mV and electrodesorption at -1000 mV with a total time of carbon polarization of about 20 days (Figure 7Sa in Supporting Information). The results showed that the single point adsorption coefficients in electrosorption dropped strongly from 860,000 L/kg in the first cycle to around 160,000 L/kg in the fifth cycle. Gineys et al. [18] studied the effect of positive and negative potentials on ACF in sodium sulfate solution as electrolyte. Under positive potentials $\leq +500$ mV, the content of oxygen-containing functional groups increased with indications for formation of phenolic and carboxylic groups. Oxidation of carbon under anodic potentials occurs either due to direct oxidation and/or from secondary reactions with more oxidizing species such as hydroxyl radicals which are produced *in-situ* at the working electrode (see Eqs. S10 to S12 in SI). Surprisingly, negative potentials on the carbon electrode lead to oxidation of the surface as well [18]. These oxidation reactions may come from secondary reactions due to reduction of dissolved oxygen producing hydrogen peroxide (Eq. S13) which can be activated by AC surfaces to hydroxyl radicals [47]. Therefore, the decrease in electrosorption of PFOA over a number of potential cycles is probably caused by advancing surface oxidation of the carbon surface, induced by the applied harsh electrosorption conditions (from +500 mV to -1000 mV).

In order to minimize carbon electrode erosion, we followed two strategies. We first tried to avoid the secondary reactions coming from the reduction of dissolved oxygen in the solution.

Therefore, we repeated the above mentioned 5 cycle electroadsorption experiment, while this time nitrogen was purged in the solution during the experiment. Again a significant drop as high as 670,000 L/kg was observed in the electroadsorption coefficient of the first cycle compared to that of the fifth cycle (Figure 7Sb). Afterwards, the electroadsorption experiment was performed with milder electrical potentials, e.g. $-100 \text{ mV} < E_{PZC} = +75 \text{ mV} < +300 \text{ mV}$ (Figure 9a). The decline in the corresponding K_d values along 10 cycles of electroadsorption is still observable but less significant (less than a factor of 2).

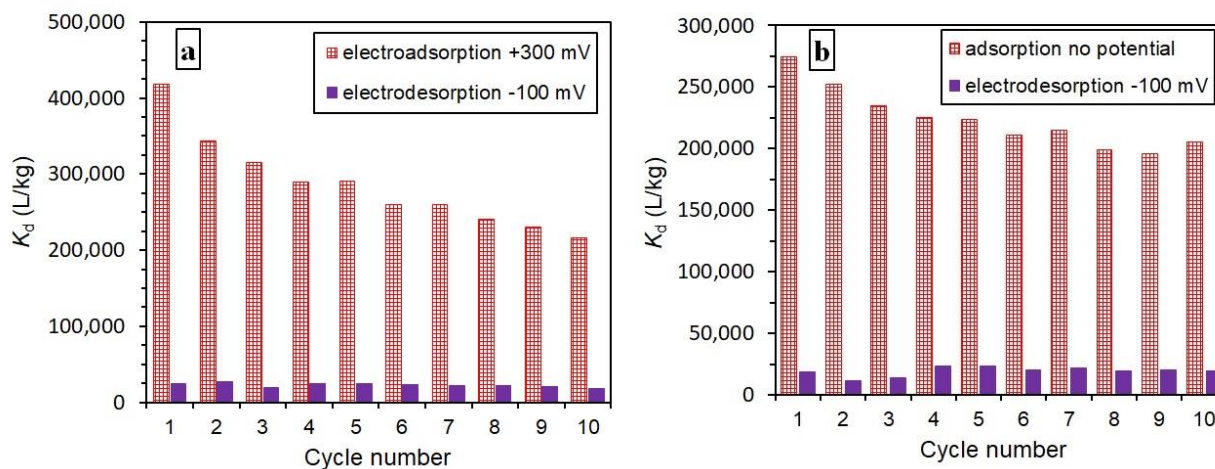


Figure 9. Electroadsorption and electrodesorption of PFOA ($C_0 = 1 \text{ mg/L}$) on/from ACF1 (66.7 mg/L) in 10 mM Na_2SO_4 at pH 7. a) 10 cycles electroadsorption at +300 mV and electrodesorption at -100 mV. b) 10 cycles adsorption without potential and electrodesorption at -100 mV. Each cycle covers 4 days, 2 days electroadsorption and 2 days electrodesorption. The potentials are versus Ag/AgCl.

Anodic polarization can be seen as more critical in terms of carbon oxidation than cathodic polarization. Bayram and Ayrancı [19] reported that cathodic polarization of ACF (by -1500 mV vs. Ag/AgCl) only slightly affected the surface chemical properties, whereas polarization with +300 mV led to a significant surface oxidation. Note that ACF1 has a high affinity towards PFOA

even without applying external potentials. Thus, in order to better protect ACF1 against attrition induced by positive potentials, PFOA adsorption can be carried out without applying an external positive potential, while a mild negative potential of -100 mV can be applied for electrodesorption.

Figure 9b illustrates the results from 10 cycles of adsorption with no external potential and electrodesorption at -100 mV over a prolonged operation time of at least 1000 h. The result is a rather stable adsorption performance of the electrosorption cell. After an initial loss of about 20% in K_d (cycle 1-5) the ACF1 electrode kept its performance almost constant (<10% decline in cycle 5-10).

4. Conclusions

External potentials were successfully used for controlling adsorption of PFOA and PFBA on microporous activated carbon felts (ACFs) with various surface chemistries. The electrosorption of both anionic compounds was influenced by the net charge on the non-polarized ACFs (studied by potential of zero charge, E_{PZC}) as well as the applied external potentials. Electrosorption of PFOA and PFBA resulted in bell-shaped curves of K_d values versus potential with maxima in K_d at potentials $> E_{PZC}$. These results indicate that for selection of appropriate carbon electrode materials, their surface chemistry and in particular their E_{PZC} should be taken into account.

The large differences between maximum K_d in electroadsorption at positive potential and K_d obtained at negative potential, e.g. 650,000 L/kg at +500 mV vs. 14,800 L/kg at -1000 mV in case of PFOA, enables one to remove the compound from a high volume of water by electroadsorption and to release it in a low volume concentrate by means of electrodesorption. An estimation of the concentration factor in an electroadsorption/-desorption unit for PFOA removal

was calculated as 115 for the conditions given above. It is lower for milder potential swings, e.g. 71 for electrosorption at +500 mV vs. -100 mV and 41 for no potential vs. -100 mV. These comparably high values encourage further studies towards the development of a continuous electroadsorption/-desorption process.

Information on E_{PZC} of carbon electrodes is also useful for protecting them against attrition caused by applying harsh potentials. Electroadsorption of PFOA at +500 mV and electrodesorption at -1000 mV showed a significant decline in electroadsorption of PFOA over 5 electroadsorption/-desorption cycles. Selection of milder potentials based on E_{PZC} of the ACF used as adsorbent (electrodesorption at -100 mV < E_{PZC} = +75mV < electroadsorption at +300 mV) resulted in only small losses of performance after 10 cycles (1000 h). An almost stable performance of the electrosorption cell was achieved without external potential for adsorption and -100 mV for electrodesorption.

The weak impact of competitive inorganic ions on electrosorption of PFBA and PFOA and a small effect of variable pH values indicate that this concept is applicable for remediation of various sources of water contaminated with both short- and long-chain perfluoroalkyl acids. Application of this procedure for remediation of water contaminated with a mix of PFAAs including sulfonates in a flow-mode is subject of our current research.

Acknowledgements

First author acknowledges funding by DAAD within NaWaM programme. We thank Merle Scherf (Leipzig University) for technical support in experiments and Prof. Dr. Volker Presser (INM – Leibniz Institute for New Materials) for providing us with the cell for EIS measurements.

References

- [1] V.A. Arias Espana, M. Mallavarapu, R. Naidu, Treatment technologies for aqueous perfluorooctanesulfonate (PFOS) and perfluorooctanoate (PFOA): a critical review with an emphasis on field testing, *Environmental Technology & Innovation* 4 (2015) 168-181.
- [2] E. Gagliano, M. Sgroi, P.P. Falciglia, F.G.A. Vagliasindi, P. Roccaro, Removal of poly- and perfluoroalkyl substances (PFAS) from water by adsorption: role of PFAS chain length, effect of organic matter and challenges in adsorbent regeneration, *Water Research* 171 (2020) 115381.
- [3] H.N. Phong Vo, H.H. Ngo, W. Guo, T.M. Hong Nguyen, J. Li, H. Liang, L. Deng, Z. Chen, T.A. Hang Nguyen, Poly- and perfluoroalkyl substances in water and wastewater: a comprehensive review from sources to remediation, *Journal of Water Process Engineering* 36 (2020) 101393.
- [4] C.P. Higgins, J.A. Field, Our Stainfree Future? A virtual issue on poly- and perfluoroalkyl substances, *Environmental Science & Technology* 51 (2017) 5859-5860.
- [5] P. McCleaf, S. Englund, A. Östlund, K. Lindegren, K. Wiberg, L. Ahrens, Removal efficiency of multiple poly- and perfluoroalkyl substances (PFASs) in drinking water using granular activated carbon (GAC) and anion exchange (AE) column tests, *Water Research* 120 (2017) 77-87.
- [6] N. Saeidi, F.-D. Kopinke, A. Georgi, Understanding the effect of carbon surface chemistry on adsorption of perfluorinated alkyl substances, *Chemical Engineering Journal* 381 (2020) 122689.
- [7] S. Deng, Y. Nie, Z. Du, Q. Huang, P. Meng, B. Wang, J. Huang, G. Yu, Enhanced adsorption of perfluorooctane sulfonate and perfluorooctanoate by bamboo-derived granular activated carbon, *Journal of Hazardous Materials* 282 (2015) 150-157.
- [8] Y. Zhi, J. Liu, Surface modification of activated carbon for enhanced adsorption of perfluoroalkyl acids from aqueous solutions, *Chemosphere* 144 (2016) 1224-1232.
- [9] M. Söregård, E. Östblom, S. Köhler, L. Ahrens, Adsorption behavior of per- and polyfluoroalkyl substances (PFASs) to 44 inorganic and organic sorbents and use of dyes as proxies for PFAS sorption, *Journal of Environmental Chemical Engineering* 8 (2020) 103744.
- [10] A. Georgi, J. Bosch, J. Bruns, K. Mackenzie, N. Saeidi, F.-D. Kopinke, Kolloidale Aktivkohle für die In-situ-Sanierung von PFAS-kontaminierten Grundwasserleitern Altlasten Spektrum 6 (2020).
- [11] Y. Zhi, J. Liu, Adsorption of perfluoroalkyl acids by carbonaceous adsorbents: effect of carbon surface chemistry, *Environmental Pollution* 202 (2015) 168-176.
- [12] X. Li, S. Chen, X. Quan, Y. Zhang, Enhanced adsorption of PFOA and PFOS on multiwalled carbon nanotubes under electrochemical assistance, *Environmental Science & Technology* 45 (2011) 8498-8505.
- [13] S. Wang, X. Li, Y. Zhang, X. Quan, S. Chen, H. Yu, H. Zhao, Electrochemically enhanced adsorption of PFOA and PFOS on multiwalled carbon nanotubes in continuous flow mode, *Chinese Science Bulletin* 59 (2014) 2890-2897.
- [14] Z. Niu, Y. Wang, H. Lin, F. Jin, Y. Li, J. Niu, Electrochemically enhanced removal of perfluorinated compounds (PFCs) from aqueous solution by CNTs-graphene composite electrode, *Chemical Engineering Journal* 328 (2017) 228-235.
- [15] K. Kim, P. Baldaguez Medina, J. Elbert, E. Kayiwa, R.D. Cusick, Y. Men, X. Su, Molecular tuning of redox-copolymers for selective electrochemical remediation, *Advanced Functional Materials* 30 (2020) 2004635.
- [16] M.A. Ahmed, S. Tewari, Capacitive deionization: processes, materials and state of the technology, *Journal of Electroanalytical Chemistry* 813 (2018) 178-192.
- [17] K.Y. Foo, B.H. Hameed, A short review of activated carbon assisted electrosorption process: an overview, current stage and future prospects, *Journal of Hazardous Materials* 170 (2009) 552-559.
- [18] M. Gineys, R. Benoit, N. Cohaut, F. Béguin, S. Delpeux-Ouldriane, Behavior of activated carbon cloths used as electrode in electrochemical processes, *Chemical Engineering Journal* 310 (2017) 1-12.
- [19] E. Bayram, E. Ayranci, A systematic study on the changes in properties of an activated carbon cloth upon polarization, *Electrochimica Acta* 56 (2011) 2184-2189.
- [20] Z. Tabti, R. Ruiz-Rosas, C. Quijada, D. Cazorla-Amorós, E. Morallón, Tailoring the surface chemistry of activated carbon cloth by electrochemical methods, *ACS Applied Materials & Interfaces* 6 (2014) 11682-11691.
- [21] P.M. Biesheuvel, S. Porada, M. Levi, M.Z. Bazant, Attractive forces in microporous carbon electrodes for capacitive deionization, *Journal of Solid State Electrochemistry* 18 (2014) 1365-1376.
- [22] G. Wang, B. Qian, Q. Dong, J. Yang, Z. Zhao, J. Qiu, Highly mesoporous activated carbon electrode for capacitive deionization, *Separation and Purification Technology* 103 (2013) 216-221.
- [23] I. Villar, S. Roldan, V. Ruiz, M. Granda, C. Blanco, R. Menéndez, R. Santamaría, Capacitive deionization of NaCl solutions with modified activated carbon electrodes, *Energy & Fuels* 24 (2010) 3329-3333.

- [24] M.A. Anderson, A.L. Cudero, J. Palma, Capacitive deionization as an electrochemical means of saving energy and delivering clean water. Comparison to present desalination practices: will it compete?, *Electrochimica Acta* 55 (2010) 3845-3856.
- [25] X. Gao, A. Omosebi, J. Landon, K. Liu, Surface charge enhanced carbon electrodes for stable and efficient capacitive deionization using inverted adsorption-desorption behavior, *Energy & Environmental Science* 8 (2015) 897-909.
- [26] I. Cohen, E. Avraham, Y. Bouhadana, A. Soffer, D. Aurbach, Long term stability of capacitive de-ionization processes for water desalination: the challenge of positive electrodes corrosion, *Electrochimica Acta* 106 (2013) 91-100.
- [27] L. Qian, A. Georgi, R. Gonzalez-Olmos, F.-D. Kopinke, Degradation of perfluorooctanoic acid adsorbed on Fe-zeolites with molecular oxygen as oxidant under UV-A irradiation, *Applied Catalysis B: Environmental* 278 (2020) 119283.
- [28] Á. Soriano, D. Gorri, A. Urriaga, Membrane preconcentration as an efficient tool to reduce the energy consumption of perfluorohexanoic acid electrochemical treatment, *Separation and Purification Technology* 208 (2019) 160-168.
- [29] A.L. Cukierman, Development and environmental applications of activated carbon cloths, *ISRN Chemical Engineering* 2013 (2013) 261523.
- [30] C. Kim, P. Srimuk, J. Lee, S. Fleischmann, M. Aslan, V. Presser, Influence of pore structure and cell voltage of activated carbon cloth as a versatile electrode material for capacitive deionization, *Carbon* 122 (2017) 329-335.
- [31] W. Chen, X. Zhang, M. Mamadiev, Z. Wang, Sorption of perfluorooctane sulfonate and perfluorooctanoate on polyacrylonitrile fiber-derived activated carbon fibers: in comparison with activated carbon, *RSC Advances* 7 (2017) 927-938.
- [32] N. Saeidi, F.-D. Kopinke, A. Georgi, What is specific in adsorption of perfluoroalkyl acids on carbon materials?, *Chemosphere* (2020) 128520.
- [33] D. Weingarth, M. Zeiger, N. Jäckel, M. Aslan, G. Feng, V. Presser, Graphitization as a universal tool to tailor the potential-dependent capacitance of carbon supercapacitors, *Advanced Energy Materials* 4 (2014) 1400316.
- [34] L.-H. Shao, J. Biener, D. Kramer, R.N. Viswanath, T.F. Baumann, A.V. Hamza, J. Weissmüller, Electrocapillary maximum and potential of zero charge of carbon aerogel, *Physical Chemistry Chemical Physics* 12 (2010) 7580-7587.
- [35] M.D. Levi, S. Sigalov, D. Aurbach, L. Daikhin, In situ electrochemical quartz crystal admittance methodology for tracking compositional and mechanical changes in porous carbon electrodes, *The Journal of Physical Chemistry C* 117 (2013) 14876-14889.
- [36] V.M. Fischer, In situ electrochemical regeneration of activated carbon, University of Groningen, Netherlands, 2001.
- [37] E. Bayram, N. Hoda, E. Ayranci, Adsorption/electrosorption of catechol and resorcinol onto high area activated carbon cloth, *Journal of Hazardous Materials* 168 (2009) 1459-1466.
- [38] A. Bán, A. Schafer, H. Wendt, Fundamentals of electrosorption on activated carbon for wastewater treatment of industrial effluents, *Journal of Applied Electrochemistry* 28 (1998) 227-236.
- [39] E. Bayram, E. Ayranci, Electrochemically enhanced removal of polycyclic aromatic basic dyes from dilute aqueous solutions by activated carbon cloth electrodes, *Environmental Science & Technology* 44 (2010) 6331-6336.
- [40] C.O. Ania, F. Béguin, Mechanism of adsorption and electrosorption of bentazone on activated carbon cloth in aqueous solutions, *Water Research* 41 (2007) 3372-3380.
- [41] S. Wang, X. Li, H. Zhao, X. Quan, S. Chen, H. Yu, Enhanced adsorption of ionizable antibiotics on activated carbon fiber under electrochemical assistance in continuous-flow modes, *Water Research* 134 (2018) 162-169.
- [42] T.D. Appleman, C.P. Higgins, O. Quiñones, B.J. Vanderford, C. Kolstad, J.C. Zeigler-Holady, E.R.V. Dickenson, Treatment of poly- and perfluoroalkyl substances in U.S. full-scale water treatment systems, *Water Research* 51 (2014) 246-255.
- [43] K.-U. Goss, The pK_a values of PFOA and other highly fluorinated carboxylic acids, *Environmental Science & Technology* 42 (2008) 456-458.
- [44] M.F. Rahman, S. Peldszus, W.B. Anderson, Behaviour and fate of perfluoroalkyl and polyfluoroalkyl substances (PFASs) in drinking water treatment: a review, *Water Research* 50 (2014) 318-340.
- [45] T.D. Appleman, E.R.V. Dickenson, C. Bellona, C.P. Higgins, Nanofiltration and granular activated carbon treatment of perfluoroalkyl acids, *Journal of Hazardous Materials* 260 (2013) 740-746.
- [46] D.N. Kothawala, S.J. Köhler, A. Östlund, K. Wiberg, L. Ahrens, Influence of dissolved organic matter concentration and composition on the removal efficiency of perfluoroalkyl substances (PFASs) during drinking water treatment, *Water Research* 121 (2017) 320-328.

[47] A. Georgi, F.-D. Kopinke, Interaction of adsorption and catalytic reactions in water decontamination processes: part I. Oxidation of organic contaminants with hydrogen peroxide catalyzed by activated carbon, *Applied Catalysis B: Environmental* 58 (2005) 9-18.